Negative Childhood Experiences Alter a Prefrontal-Insular-Motor Cortical Network in Healthy Adults: A Preliminary Multimodal rsfMRI-fMRI-MRS-dMRI Study

Niall W. Duncan,[1,2,3,4]* Dave J. Hayes,[5] Christine Wiebking,[6] Brice Tiret,[7] Karin Pietruska,[8] David Q. Chen,[5] Pierre Rainville,[8] Małgorzata Marjańska,[9] Omar Ayad,[1] Julien Doyon,[7] Mojgan Hodaie,[5] and Georg Northoff[1,2,3,4]

[1]Graduate Institute of Humanities in Medicine, Taipei Medical University, Taipei, Taiwan
[2]Brain and Consciousness Research Center, Taipei Medical University-Shuang Ho Hospital, New Taipei City, Taiwan
[3]Centre for Cognition and Brain Disorders, Hangzhou Normal University, Hangzhou, China
[4]Mind, Brain Imaging and Neuroethics Research Unit, Institute of Mental Health Research, University of Ottawa, Ottawa, Canada
[5]Division of Neurosurgery, Department of Surgery, University of Toronto and Division of Brain Imaging and Behaviour Systems Neuroscience, Toronto Western Research Institute, Toronto, Ontario, Canada
[6]Cluster of Excellence in Cognitive Sciences, Department of Sociology of Physical Activity and Health, University of Potsdam, Potsdam, Germany
[7]Functional Neuroimaging Unit and Department of Psychology, Université de Montréal, Montréal, Canada
[8]Faculté de médecine dentaire, Université de Montréal, Montréal, Canada
[9]Center for Magnetic Resonance Research and Department of Radiology, University of Minnesota, Minneapolis, Minnesota

◆ ═══════════════════════════════ ◆
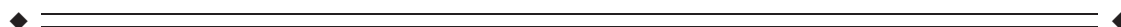
Abstract: Research in humans and animals has shown that negative childhood experiences (NCE) can have long-term effects on the structure and function of the brain. Alterations have been noted in grey and white matter, in the brain's resting state, on the glutamatergic system, and on neural and behavioural responses to aversive stimuli. These effects can be linked to psychiatric disorder such as depression and anxiety disorders that are influenced by excessive exposure to early life stressors. The aim of the current study was to investigate the effect of NCEs on these systems. Resting state functional MRI (rsfMRI), aversion task fMRI, glutamate magnetic resonance spectroscopy (MRS), and diffusion magnetic resonance imaging (dMRI) were combined with the Childhood Trauma Questionnaire (CTQ) in

healthy subjects to examine the impact of NCEs on the brain. Low CTQ scores, a measure of NCEs, were related to higher resting state glutamate levels and higher resting state entropy in the medial prefrontal cortex (mPFC). CTQ scores, mPFC glutamate and entropy, correlated with neural BOLD responses to the anticipation of aversive stimuli in regions throughout the aversion-related network, with strong correlations between all measures in the motor cortex and left insula. Structural connectivity strength, measured using mean fractional anisotropy, between the mPFC and left insula correlated to aversion-related signal changes in the motor cortex. These findings highlight the impact of NCEs on multiple inter-related brain systems. In particular, they highlight the role of a prefrontal-insular-motor cortical network in the processing and responsivity to aversive stimuli and its potential adaptability by NCEs. *Hum Brain Mapp 36:4622–4637, 2015.*   © 2015 **Wiley Periodicals, Inc.**

Key words: affect; early life stress; brain networks; aversion; resting state; mood disorder

◆ ━━━━━━━━━━━━━━━━━━━━━━━━━━━━━━━ ◆

INTRODUCTION

Negative childhood experiences (NCEs) are prevalent in society and have been linked to a broad range of mental health problems in adulthood [Edwards et al., 2003; Kuo et al., 2011; Nelson et al., 2002; Turecki et al., 2012]. A growing body of studies indicates that NCEs can lead to alterations in brain structure and function in both healthy and clinical populations. For instance, brain imaging studies have correlated NCEs to changes in both task-related [Grant et al., 2011; Mueller et al., 2010; Thomaes et al., 2012] and intrinsic (or resting state) brain activity [Bluhm et al., 2009; McFarlane et al., 2005]. One particular psychometric measure of NCEs, the childhood trauma questionnaire (CTQ) – which has been shown to be a reliable measure of physical-emotional abuse and neglect in healthy populations [Paivio and Cramer, 2004] – has been correlated to alterations in cognitive function [Gould et al., 2012; Majer et al., 2010], neuroendocrine stress responses [Carpenter et al., 2011], microstructural white matter [Lu et al., 2013], as well as resting state [Howells et al., 2012] and emotion-related [Dannlowski et al., 2012] brain function in healthy humans. These results suggest that NCEs, even in healthy adults, can predict changes in brain structure, function, and behavior.

The medial prefrontal cortex (mPFC) is the main anterior region of the default-mode resting state network but is also integral for the processing of many tasks. In particular, recent studies have shown that mPFC rest- and task-related brain connectivity and function are correlated to the response of the hypothalamic-pituitary stress axis [Kiem et al., 2013] and aversion-related brain activity [Hayes et al., 2013, 2014] and is likely key in contextualizing emotion-related information [Roy et al., 2012]. For instance, prior studies in humans and animals have revealed a common network of aversion-related activity, which includes the mPFC, insula, motor cortex, posterior and mid cingulate, thalamus, amygdala, orbitofrontal cortex, nucleus accumbens, and midbrain [Hayes et al., 2011, 2014]. Although there are few studies specifically looking at the relationship of the mPFC to the rest of this network,

one recent study has shown that a measure of GABA in the mPFC is correlated to BOLD activity both within the mPFC itself as well as in the motor cortex during aversive responding [Hayes et al., 2013].

Moreover, a history of NCEs in healthy, medication-free, adults is predictive of reduced resting state functional connectivity and greater blood oxygen level-dependent (BOLD) task-related deactivations within regions of the default-mode network, including the mPFC [Philip et al., 2013a,b]. Biochemically, the function of the mPFC glutamatergic system has been tied to differences in intrinsic brain activity in humans [Duncan et al., 2011, 2013, 2014] as well as aberrant neural and behavioral outcomes related to the effects of early life stress in rodents [Ali et al., 2011; Judo et al., 2010; Llorente et al., 2012]. Measures of entropy [Bruce et al., 2009; Richman and Moorman, 2000], which reflect intraregional functional variability across time, are of particular interest as the complexity of brain activity has been shown to alter during development and has been linked to efficient brain function [Garrett et al., 2013; Misić et al., 2010]. Together, these data underscore the need to better describe the relationship between NCEs and the structure and function of the mPFC in healthy humans.

An investigation of this nature would be especially relevant to prior work showing blunted neural responding to aversive stimuli and altered affective circuitry in animal models of early life stress [Howell et al., 2013; Jahng et al., 2010] and in humans with mood and anxiety disorders [Etkin and Wager, 2007; Liberzon et al., 2007; Shin et al., 2004; Shin and Handwerger, 2009; van Tol et al., 2012]. Moreover, the presence of NCEs has been associated with decreased PFC grey matter and altered PFC white matter connectivity [Hanson et al., 2012]. Based on dysfunctions in the default-mode network and emotional brain function in a range of mental health problems associated with NCEs, including post-traumatic stress disorder, major depressive disorder and anxiety disorders, a connection between aberrant default-mode network development and mental disorders in adulthood has been proposed [Broyd et al., 2009; Daniels et al., 2011; Northoff et al., 2011].

The main aim of this study was to investigate the link between NCEs, measured with the CTQ [Bernstein et al.,

1994; Paivio and Cramer, 2004], and brain structure and function. To this end, we used a multimodal neuroimaging approach including a combination of functional magnetic resonance imaging (fMRI), magnetic resonance spectroscopy (MRS), and diffusion magnetic resonance imaging (dMRI) to explore whether NCEs were related to glutamate levels, BOLD activity, and white matter connectivity associated with the mPFC. Importantly, our goal was to explore the relationship of the mPFC to NCEs and aversive brain activity, not explicitly as a member of the default-mode network, but as a hub of affective network activity. Based on the prior animal and human work noted above, the first hypothesis was that higher CTQ scores, reflecting more NCEs, would correlate with disruptions in mPFC resting state activity (i.e. increased signal variability, or entropy, across time) and decreased glutamate levels. The second hypothesis was that more NCEs would result in reduced neural reactivity within the aversion-related network [Hayes et al., 2011, 2014], noted above, to the anticipation of aversive stimuli and that this blunted activity would be correlated with disruptions in white matter connectivity to the mPFC.

METHODS

Twenty-five healthy, right-handed participants (9 female; 22 ± 3.9 years) were scanned using MRI and MRS at two different scan centres (resting state fMRI, rsfMRI, and diffusion MRI, dMRI – Montreal Neurological Institute, McGill University; aversion fMRI and MRS – Unité de neuroimagerie fonctionelle, Université de Montréal). Aversion fMRI and MRS scans were carried out on the same day. Siemens 3T Trio scanners were used at both locations. Mean time between the two scan days was 3.6 days (range = 1–10 days). Participants were screened for current or past psychiatric or neurological disorders and current recreational drug use through a semi-structured interview. Screening for depression was carried out using the Beck Depression Inventory, with a cut-off score greater than or equal to four [Beck et al., 1996]. Participants were also excluded if they were currently using any medication other than contraceptives or were heavy alcohol users (i.e. more than two drinks per day). Participant demographic details can be found in the Supporting information.

Data from a number of participants were excluded because of incorrectly completed questionnaires, excessive head-motion during any modality, drowsiness during rest [Duncan and Northoff, 2012], or unusable MRS results. This strict quality control left a final group of twelve participants that completed all imaging modalities and psychological testing (6 female, 23 ± 3.5 years), although one additional subject was removed from the diffusion MRI analysis because of incomplete data. Beyond the core 12 subjects, analyses combining each relevant modality were also carried out using the maximal number of participants where possible (Supporting Information material); these
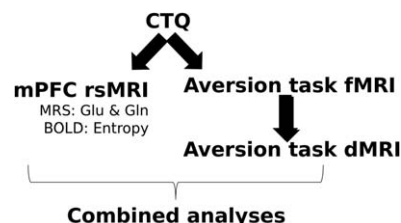

Figure 1.
Overview of study design.

supplementary results all support the findings from this core group of 12. For these supplementary analyses 20 subjects had usable mPFC MRS data, 19 had usable left insula (Lins) MRS data, and 15 had usable resting state data. All participants gave their written informed consent and were compensated financially. Approval for the study was obtained from the ethics committees at McGill University and the Université de Montréal. Independent analyses of this dataset have been published previously [Duncan et al., 2013] and [Hayes et al., 2013].

Psychological Scales

Participants completed the CTQ and the Anxiety Sensitivity Index (ASI) [Reiss et al., 1986]. Total CTQ scores were used throughout, as it has been shown to be a stable and reliable indicator of NCEs, both in general and in the specific population studied [Bernstein et al., 1994; Paivio and Cramer, 2004]. Participants also completed the Marlowe-Crowne Social Desirability Scale, to determine if questionnaire responses were influenced by a propensity to adhere to social norms [Fraboni and Cooper, 1989].

Magnetic Resonance Spectroscopy

Single voxel edited ^{1}H MR spectra were acquired using the MEGA-PRESS method [Marjanska et al., 2007; Mescher et al., 1998]. Voxels of interest were located in the mPFC ($48 \times 21 \times 21$ mm^3) and the left insula ($23 \times 48 \times 27$ mm^3) (Supporting Information Fig. 1 for locations). Difference spectra were analysed using LCModel 6.2-1A [Provencher, 1993, 2001] using a basis set that included an experimentally measured metabolite-nulled macromolecular spectrum from the occipital cortex (average from 10 subjects) and the experimentally measured spectra from 100 mM phantoms of N-acetylaspartate (NAA), creatine, γ-aminobutyric acid (GABA), glutamate (Glu), and glutamine (Gln) with pH adjusted to 7.2 and at 37℃. Only results with the Cramer-Rao lower bounds (CRLB) below 20% were included in the analysis. Concentrations with CRLB > 20% were classified as not detected. The mPFC, centred on the perigenual anterior cingulate cortex, was the target region for the study and the LIns was used as a comparative region, given its clear involvement in aversive responding and our hypotheses that it would show

aversion-related BOLD activity without acting as a key modulator of the network (e.g. its resting activity or neurochemical content would not correlate to changes in other regions of the network). Moreover, the left insula was chosen over the right as it is known to play a greater role in affective responding [Duerden et al., 2013]. Metabolites were expressed in relation to NAA concentrations.

fMRI Parameters and Preprocessing

Resting state functional echo planar image (EPI) scans were acquired using body coil transmit and a 32-channel headcoil. Forty-seven slices aligned at $-30°$ from the AC-PC plane and covering the whole brain were acquired per volume (FoV = 205 $\times$ 205 mm^2; spatial resolution = 3.2 $\times$ 3.2 $\times$ 3.2 mm^3; TE = 25 ms; TR = 2,270 ms; flip angle = 90°). The first five volumes were discarded. A high-resolution anatomical image was also acquired (MPRAGE; spatial resolution = 1 $\times$ 1 $\times$ 1 mm^3). Aversion task EPI scans were carried out using the same acquisition parameters as the resting state other than the inclusion of a gap between each volume acquisition of 400 ms. This gap was included to allow the collection of shock response EMG data without the presence of confounding scanner electromagnetic noise [Piché et al., 2010]. The EMG data were not included in the present analysis.

The processing of fMRI data was carried out with the FSL suite of tools [Smith et al., 2004]. In preprocessing steps common to both the rest and aversion tasks, functional images were aligned to the middle volume, slice time corrected, and high-pass filtered (100 s). Functional and anatomical images were aligned with the FSL MNI standard space template using nonlinear transformations.

Resting State Functional MRI

The resting state session consisted of two eyes-open (EO) and two eyes-closed (EC) periods (2 $\times$ 120 s each), counterbalanced across participants and indicated with short tones. EO and EC resting state scans were considered separately given prior findings of differences between the two conditions [Qin et al., 2012]. Participants were monitored using a simple camera setup to ensure that they followed the task and to monitor levels of drowsiness [Duncan and Northoff, 2012].

Individual resting state data was submitted to an independent component analysis from which noise components (head motion, blood and breathing related signals) were identified by two independent investigators [Kelly et al., 2010] and regressed out of the unsmoothed data, along with the six head-motion parameters. Again, the primary region of interest was the mPFC MRS voxel, with the LIns MRS voxel serving as a task-positive comparative region. MRS regions were individually masked to create grey matter regions-of-interest (ROIs) from each subject. The binary grey matter masks were produced by segmenting each subject's anatomical image and thresholding the resulting grey matter maps at a probability of 0.95. mPFC and LIns grey matter ROIs (mean volume = 3926 $\pm$ 1108 mm^3; 8492 $\pm$ 1153 mm^3, respectively) were converted into functional space using nonlinear transformations. The timecourse from each ROI was extracted from the unsmoothed data for the EO and EC periods.

Mean ROI entropy was calculated using the SampEn toolbox for MATLAB [Richman and Moorman, 2000] by determining the measure for each voxel and then averaging across the whole ROI. The SampEn method gives a nonlinear characterization of the degree of organisation within a timeseries, in this case the BOLD signal [Aboy et al., 2007; Hauge et al., 2011]. This is done by calculating the log likelihood that a series of points of a length m (at a particular matching threshold, r) will also be the same at a length of $m + 1$ [Richman and Moorman, 2000], as calculated for all sets of points in the timecourse. An increase in entropy is generally associated with an increase in signal complexity [Costa et al., 2005]. Timecourses were normalized to have a mean of 0 and variance of 1 prior to entropy calculation. A template length of $m = 2$ and a matching threshold of 20% of the standard deviation of the original timecourse ($r = 0.2$) was used.

Aversion Task

Participants underwent an aversion task as reported previously [Hayes et al., 2013]. Electric shocks were applied to the left ankle using parameters reported elsewhere [Ladouceur et al., 2012; Mailhot et al., 2012]. Stimulation (10 $\times$ 1 ms rectangular pulses; rate = 333 Hz, train duration = 30ms; <25 mA) was administered to the skin over the retromalleolar path of the sural nerve at the ankle via custom-made surface electrodes (1cm^2; spaced 2 cm apart) using an isolated DS7A constant current stimulator (Digitimer, Welwyn Garden City, Hertfordshire, UK) and triggered by a Grass S88 train generator (Grass Medical Instruments, Quincy, MA, USA). Stimulation intensity was individually determined in a mock scanner using the staircase method [Willer, 1977], with shocks during the experiment being applied at an intensity of 120% of the participant's pain threshold. The subjective experience of pain ratings (0–100, where 0 is not painful and 100 is the worst imaginable pain) averaged 50.65 $\pm$ 13.26 across all subjects, consistent with mild to moderate levels of pain [Mailhot et al., 2012]. Real-time visual inspection of electrodermal activity was used as further validation that the stimulation was unpleasant.

The event-design task focused on the anticipation of aversion. At the start of each trial subjects were indicated (0.5 s) as to whether they would receive a shock with 100% certainty (certain aversion), with 33% certainty (uncertain aversion), or whether they would receive no shock (safe). This indicator was followed by a first anticipation period (4–8 s) and then a tone presentation period (2 s). Prior to scanning, two tones were either conditioned to an aversive stimulus (i.e., white noise startle), or were presented in the absence of the startling noise (i.e., was neutral). Following the tone was

a second anticipation period (4–8 s), and finally a shock delivery in the relevant trials. The order of trials was pseudo-randomized and intertrial intervals (1–3 s) were interspersed pseudo-randomly amongst trials. Each condition was presented 25 five times over four runs, giving a total scan time of ∼50 minutes. Results from the tone conditioning are presented elsewhere [Hayes et al., 2013]. As only the anticipation period was of interest in the present study, given its sensitivity to individual differences in aversive responses [Carlson et al., 2011], a simplified analytical approach was used, whereby the anticipation periods were collapsed across tone types leaving only the aversive anticipation periods delineating the certain shock, uncertain shock, and safe conditions.

Following preprocessing, aversion functional data were smoothed (5 mm FWHM kernel) and then analyzed using a standard GLM approach, as implemented in FEAT [Smith et al., 2004]. All events were convolved with a canonical double-gamma HRF. Head-motion parameters and the mean signal from the CSF and white matter were included as nuisance variables. As the target was aversive responses, the contrasts of interest were the anticipation of certain aversion (ACA) versus the anticipation of no shock (Safe), [ACA v Safe], and the anticipation of uncertain aversion (AUA) versus the anticipation of no shock, [AUA v Safe].

Diffusion Magnetic Resonance Imaging

Diffusion magnetic resonance (dMRI) images were acquired using an 8-channel phased-array headcoil. They were acquired using 99 non-collinear directions over an 8 min 51 s period with a single-shot spin-echo echo planar sequence, using the following parameters: 1.9 mm isovoxel, 64 slices, 128×128 matrix, FOV $= 243 \times 243$ mm^2, TE $= 89$ ms, TR $= 8.3$ s, Fourier factor $= 6/8$, b $= 1,000$ s/mm^2, 10 acquisitions with $b = 0$, with GRAPPA parallel reconstruction with an acceleration factor of 2. The FSL v 5.0 suite (FMRIB Software Library, http://fmrib.ox.ac.uk/fsl) [Smith et al., 2004] and 3D Slicer v 4.3.1 (NA-MIC©, http://www.slicer.org) [Fedorov et al., 2012] suite of brain imaging tools in a Linux environment were used for preprocessing, registration, and analyses. Diffusion-weighted scans were motion- and eddy-current corrected in FSL and imported to 3D Slicer for T1 to mean diffusion-weighted baseline linear registration and visualization, tensor estimation and the creation of scalar maps for fractional anisotropy (FA) at the individual level. As recommended by others [Leemans and Jones, 2009], we corrected the b-matrices with finite strain correction by averaging the rotational component of the gradient affine transforms and then applied these to the original b-matrices.

Whole-brain deterministic multitensor tractography was performed using the eXtended Streamline Tractography, or XST, algorithm implemented in 3D Slicer [Qazi et al., 2009]. This approach was chosen over others given its superior ability to discern dense, crossing, highly angled,

and long-distance traveling fibres [Descoteaux et al., 2009; Khalsa et al., 2014; Qazi et al., 2009]. The seed regions for tractography were the overlapping mPFC, motor cortex, and left insula regions noted from the combined multimodal neuroimaging analyses (see below). All analyses were performed in individual-subject space. The grey matter seed regions were transformed from MNI space to individual space, a Gaussian blur of 1mm was applied so that the masks expanded slightly to include the surrounding white matter, and then binarized and resampled to individual diffusion-weighted space.

Multitensor tractography models were generated using the following parameters: 0.25 mm seed spacing, C_1 threshold $= 0.2$, tensor fractional $= 0.1$, curve radius $= 0.8$ radians, minimal path length $= 10$ mm, step size of 1 mm. See Qazi et al. [2009] for an in-depth description of parameters. Resulting tracts were then binarised to voxel space (i.e. assigned a value of 1 if a streamline passed through it and zero if it did not), and the conjunction of multitensor maps between the regions (Motor ∩ mPFC; mPFC ∩ Insula; Motor ∩ Insula) were identified using fslmaths. Connectivity was inferred by the presence of common voxels between each ROI pair. A connection between two regions was inferred to be 'direct' when overlapping voxels were found within each pair of ROIs or was within three voxels of both ROIs, and was considered 'not direct' when at least one ROI did not have white matter voxels which met these conditions. The fractional anisotropy of these common maps was extracted as an indicator of the strength of structural connections between each pair of ROIs [Ben-Shachar et al., 2007; Khalsa et al., 2014]. However, it is important to note that the term 'structural connectivity' refers to the apparent connections between these three regions as identified by the multitensor models, and that biological connectivity is inferred but not guaranteed [Le Bihan and Johansen-Berg, 2012].

Combination of Measures

The overall multimodal design of the study is outlined in Figure 1. Overall, the purpose of combining such measures was to investigate the potential impact of self-reported NCEs (i.e. CTQ scores) on mPFC structure and function and on whole-brain aversion-related activity. As such, two lines of analysis were performed: (1) CTQ was correlated to the mPFC's baseline BOLD activity – i.e. resting state or rsfMRI, which was measured here via entropy—and its potential for excitation —i.e. which is indirectly measured through MRS measures of glutamate, the brain's primary excitatory neurotransmitter; (2) CTQ was correlated to the whole-brain aversion-related BOLD activity (i.e. via the fMRI design outlined above) and then to the indirect measure of structural connectivity strength (i.e. extracting fractional anisotropy from white matter pathways identified by multi-tensor tractography) between the three regions identified in the previous analyses. Although reliant on correlations, this multimodal approach is currently the best method for linking behavior

TABLE I. Summary of correlation analyses between CTQ scores and (A) anxiety scores, (B) mPFC and left insula Glx and Glu ratios, and (C) mPFC and left insula resting state measures for eyes-open and eyes-closed rest

	Correlation coefficient (95% C.I.), P-value	
(A) [inc. age + SocDes]		
CTQ × ASI ($n = 25$)	**0.70, $P < 0.001$**	
CTQ × ASI ($n = 12$)	0.53, $P = 0.072$	
	mPFC	**Left insula**
(B) [inc. age]		
CTQ × Glx/NAA	-0.23 ($-0.74 - 0.33$), $P = 0.35$	0.17 ($-0.45 - 0.67$), $P = 0.67$
CTQ × Glu/NAA	**-0.64 ($-0.91 - 0.23$), $P = 0.009$**	0.25 ($-0.35 - 0.71$), $P = 0.40$
(C) [inc. age]		
CTQ × Ent EC	**0.80 ($0.43 - 0.94$), $P = 0.002$**	0.25 ($-0.35 - 0.71$), $P = 0.40$
CTQ × Ent EO	0.23 ($-0.33 - 0.68$), $P = 0.41$	0.31 ($-0.54 - 0.65$), $P = 0.33$

Abbreviations: CTQ, childhood trauma questionnaire; SocDes, social desirability scale; ASI, anxiety sensitivity index; mPFC, medial prefrontal cortex; Glu/NAA, glutamate/NAA; Glx/NAA, glutamate+glutamine/NAA; Ent, sample entropy.

with *in vivo* measures of brain function, chemistry, and structure in humans.

Relationships between the basic measures (psychological scores, biochemistry, structural connectivity, and entropy values) were tested using Pearson correlation or partial correlation analyses where appropriate. To determine the relationship between brain responses to the anticipation of aversion and each of the psychological scores, the entropy values, and mPFC Glu/NAA, whole-brain regression analyses were carried out at the group level in FSL's FEAT. Significance for all analyses was set at $P < 0.05$. As multiple statistical comparisons were made, steps were taken to control for this – FDR correction was used in the case of correlation results (uncorrected $P < 0.009$) [Benjamini and Hochberg, 1995] and cluster-based FWE correction for whole-brain analyses ($Z > 2.3$) [Woolrich et al., 2009].

RESULTS

Results from the participant group in which all modalities were available ($n = 12$) are given here unless stated otherwise. Supporting results from separate participant subgroups that maximize the sample size for each component can be found at the end of each respective section and conform to those from the core group of 12.

CTQ Correlates with mPFC Glutamate and Resting State Measures

No individual had a subscale score (emotional abuse/neglect, physical abuse/neglect, sexual abuse) in the severe range, although the total CTQ scores (37 ± 5.1; range: 28–44) are consistent with subjects reporting low to moderate levels of NCEs [Lu et al., 2013]. CTQ scores were positively correlated with ASI scores in the whole group ($n = 25$), controlling for subject age and social desirability scale scores, although this was a trend in the $n = 12$ subgroup (Table IA).

As hypothesized, CTQ scores correlated negatively with mPFC Glu/NAA concentrations ($n = 12$), although not with Glx/NAA levels (Fig. 2A, Table IIB). In contrast, CTQ scores were not correlated with biochemical measures in the LIns control region. As anxiety disorders have been linked to changes in NAA levels in the mPFC [Shin and Liberzon, 2010], NAA levels in the mPFC were correlated with CTQ scores. No relationship was seen ($n = 20$, $R = 0.11$, $P = 0.66$). A group of 20 participants had both usable CTQ scores and usable mPFC MRS results. CTQ scores were negatively correlated with mPFC Glu/NAA ($n = 20$, $R = -0.57$, $P = 0.009$) but not correlated with mPFC Glx/NAA ($n = 20$, $R = -0.14$, $P = 0.57$). In the LIns, 19 participants had both CTQ and MRS data. No relationship between CTQ scores and LIns Glu/NAA ($n = 19$, $R = -0.17$, $P = 0.47$) or Glx/NAA ($n = 19$, $R = 0.05$, $P = 0.84$) was seen.

Resting state entropy within the mPFC ROI during the eyes-closed condition was found to correlate positively with CTQ scores (Fig. 2B; Table IC). During the EO condition, no correlation was observed. No correlation was found between the CTQ scores and entropy in the LIns during either EO or eyes-closed (Table IC). Fifteen participants had usable resting-state and CTQ data. A positive correlation between CTQ scores and mPFC eyes-closed entropy was seen ($n = 15$, $R = 0.72$, $P = 0.0039$). A trend was seen with eyes-open entropy ($n = 15$, $R = 0.48$, $P = 0.08$).

Left Insula and Motor Cortex Activity Correlate with Aversion BOLD, CTQ, Glutamate, and rsfMRI

The main results from this section are all illustrated in Figure 3.

Aversion BOLD and CTQ

The aversion task produced responses consistent with previous studies [Fig. 3A; Hayes and Northoff, 2011]. Anticipation of certain aversion (ACA) induced strong
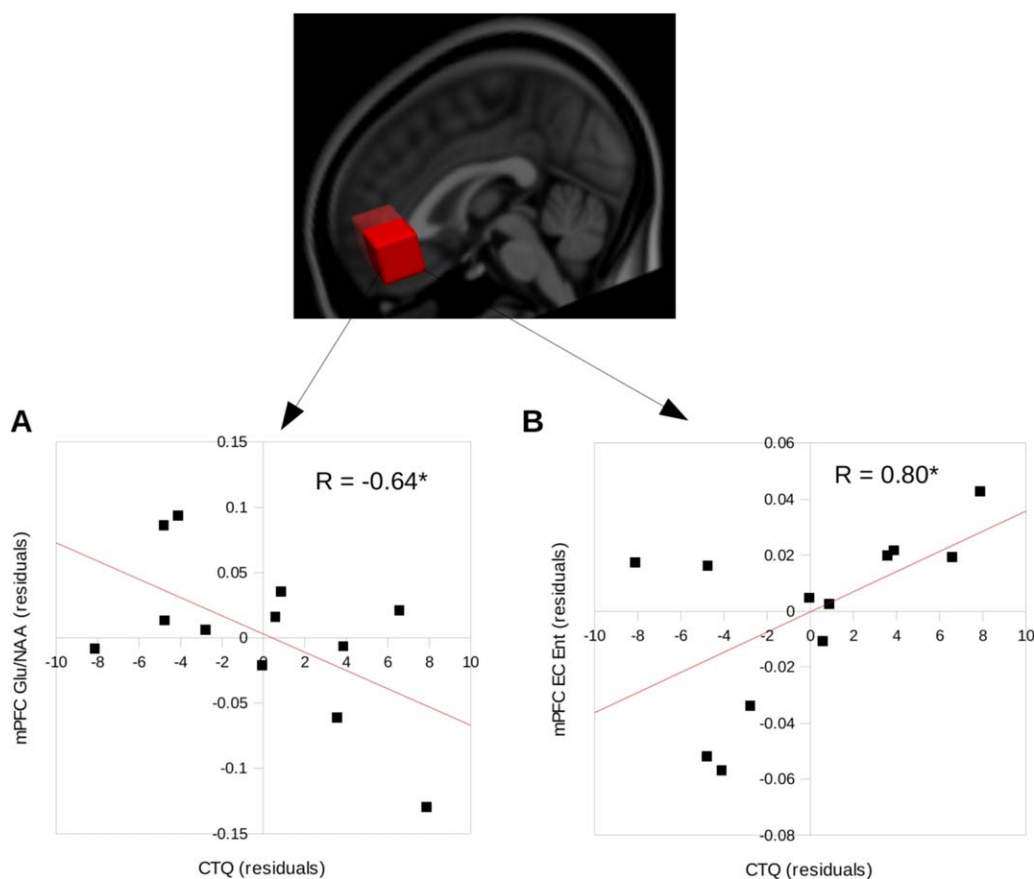
Figure 2.
(A) Correlation between CTQ scores and mPFC Glu concentrations and (**B**) between CTQ scores and mPFC entropy during eyes-closed condition, both controlling for subject age. * denotes $P_{FDR} < 0.05$. [Color figure can be viewed in the online issue, which is available at wileyonlinelibrary.com.]

responses in, amongst other regions, the sensorimotor cortex and bilateral insula (Fig. 3A, Supporting Information Table S2A). Anticipation of uncertain aversion (AUA) induced similar responses, although of a lesser extent (Supporting Information Fig. S2A, Table S2B). During ACA, the response to the anticipation of aversion was found to correlate negatively with CTQ scores in multiple areas, primarily the PCC, sensorimotor cortex and left insula (Fig. 3B, Supporting Information Table S3A). The BOLD response to AUA was also found to correlate negatively with CTQ scores in the PCC and precuneus (Supporting Information Figure S2B and Table S3B).

Aversion BOLD and biochemistry

Although no correlations were noted at the FWE corrected level, Glu/NAA in the mPFC correlated positively with the response to ACA (but not AUA) in the sensorimotor cortex and left insula at a more lenient threshold of 0.005, uncorrected (Fig. 3C, Supporting Information Table S3). We believe that a lowered threshold is justified for this measure, given our *a priori* hypotheses, the low subject number, and the lower signal-to-noise ratio inherent in MRS measurements. Importantly, no other significant correlations were noted with the ACA or AUA maps at either threshold for any other biochemical measures, including with mPFC Glx/NAA, LIns Glx/NAA, and LIns Glu/NAA. Also, none of the other analyses involved reduced statistical thresholding of any kind.

Aversion BOLD and rsfMRI

Entropy in the mPFC during EC was found to correlate negatively with ACA responses in the insula and motor cortex (Fig. 3D, Supporting Information Table S4A). The response to AUA was found to correlate negatively with mPFC eyes-closed entropy in the sensorimotor cortex and precuneus (Supporting Information Fig. S2D and Table S4B). No relationship was found between the ACA or AUA BOLD and mPFC eyes-open entropy.

TABLE II. (A) Pearson correlations for mean fractional anisotropy of overlapping white matter voxels identified for each ROI pair (i.e. Motor ∩ mPFC; mPFC ∩ Ins; Motor ∩ Ins)

		% Sig change difference during ACA		
		Motor − mPFC (r, p)	mPFC − Ins (r, p)	Motor − Ins (r, p)
Mean FA	Motor ∩ mPFC	−0.08, 0.81	0.114, 0.74	−0.002, 0.99
	mPFC ∩ Ins	0.53, 0.09	−0.102, 0.77	**0.72, 0.012**
	Motor ∩ Ins	0.05, 0.88	−0.03, 0.94	0.06, 0.87

		% Sig change during ACA		
		mPFC	Insula	Motor
Mean FA	mPFC ∩ Ins	−0.098, 0.77	0.038, 0.91	**0.675, 0.023**
		CTQ Scores		
Mean FA	mPFC ∩ Ins	−0.198, 0.56		

% signal change difference for the same ROI pair during the anticipation of certain aversion (ACA); (B) the significant mPFC-Ins pair and the % signal change in each region of the mPFC, insula and motor cortex; (C) the significant mPFC-Ins pair and CTQ scores.
Significant correlations are highlighted in bold
FA = mean fractional anisotropy; p = p-values; r = Pearson's correlations.
Abbreviations: ASI, anxiety sensitivity index; CTQ, childhood trauma questionnaire; EPI, echo planar image; mPFC, medial prefrontal cortex; MRS, magnetic resonance spectroscopy; NCEs, negative childhood experiences; rsfMRI, resting state functional MRI

Aversion BOLD and CTQ, biochemistry and rsfMRI

Results from each of the regressions with ACA activity were combined to visually identify regions in which all overlap, highlighting the motor cortex and left insula (Fig. 3E). The overlapping regions in the motor cortex and left insula consisted of 157 voxels (2 × 2 × 2 mm^3) and 27 voxels, respectively. To further typify the CTQ effect on aversion responses in these overlapping regions, signal changes for the individual conditions (Safe, AUA, and ACA) were extracted from the motor cortex overlap. These were then correlated with CTQ scores, showing that the negative correlation with [ACA > Safe] activity is driven by a reduced ACA response, rather than increased safe signal changes (Fig. 3F).

Structural Connectivity Between mPFC and Left Insula Is Related to Aversive Motor Cortex Signal Changes

Figure 4A-B shows an example of the multitensor tractography models generated for an individual. All subjects showed connectivity between the three pairs of ROIs identified by the multimodal (i.e. MRS, fMRI, CTQ) analysis, resulting in three connectivity maps (i.e. Motor ∩ mPFC; mPFC ∩ Insula; Motor ∩ Insula). Most subjects also showed evidence of 'direct' connectivity (eight for Motor ∩ mPFC; seven each for mPFC ∩ Insula and Motor ∩ Insula; see Methods for definition). Connectivity strength

(i.e. mean fractional anisotropy) from each subject's connectivity maps (see Supporting Information Table 6 for values) was correlated with the difference in percent (%) signal changes during the ACA condition between each ROI pair (Table IIA), revealing a correlation between mPFC ∩ Insula connectivity strength and the difference in motor cortex and left insula % signal changes (Table IIA, Fig. 4C; r = 0.72, P = 0.012). Further investigation revealed that this correlation was driven by the relationship between mPFC ∩ Insula connectivity strength and percent signal changes in the motor cortex (Table IIB, Fig. 4D; r = 0.68, P = 0.023) during the anticipation of aversive stimuli, but was not related to signals in the left insula (r = 0.04, P = 0.91) or mPFC (r = −0.10, P = 0.77) (Table IIB; Fig. 4D). mPFC ∩ Insula FA was not correlated with CTQ scores (Table IIC; r = −0.198, p = 0.56); nor did CTQ correlate with FA values extracted from the mPFC ∩ Motor (r = −0.252, p = 0.45) or Motor ∩ Insula (r = 0.161, P = 0.64) tractography maps.

DISCUSSION

We used a multimodal neuroimaging approach to investigate the potential relationship between reports of negative childhood experiences (NCEs; measured using the CTQ) and changes in brain structure and function (Fig. 1). Consistent with our first hypothesis, higher CTQ scores (reflecting more NCEs) were found to correlate negatively with mPFC resting state Glu/NAA levels and positively
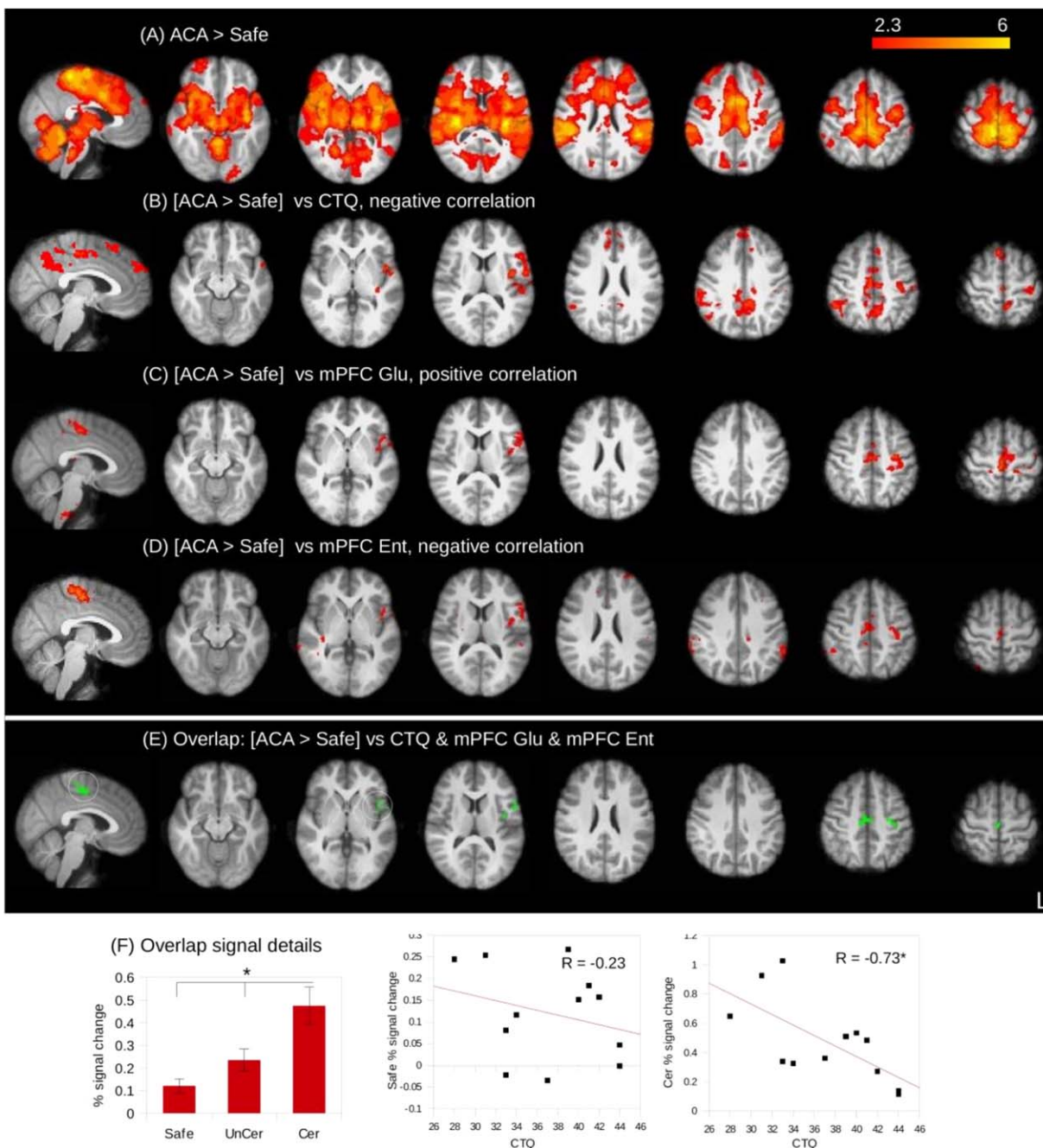
Figure 3.

Brain maps showing (**A**) the basic contrast of the anticipation of certain aversion > safe [ACA > Safe]; (**B**) the negative correlation between [ACA > Safe] contrast values and CTQ scores (controlling for ASI); (**C**) the positive correlation between [ACA > Safe] contrast values and mPFC Glu; (**D**) the negative correlation between [ACA > Safe] contrast values and mPFC entropy; and (**E**) the overlap, in green, between each of these maps. Details of safe and certain individual condition percent signal changes from the overlap in the sensorimotor cortex are given, showing that CTQ scores are correlated with a decrease in Certain signal change (**F**). Image result threshold is $P < 0.05$, FWE corrected ($n = 12$), other than [ACA > Safe] vs mPFC Glu/ NAA where it is $P < 0.005$, uncorrected. Results are shown superimposed on the study mean anatomical image. * indicates $P_{FDR} < 0.05$. Sagittal $x = 4$. CTQ, childhood trauma questionnaire; mPFC, medial prefrontal cortex; Glu/NAA, glutamate/ NAA; Ent, sample entropy. [Color figure can be viewed in the online issue, which is available at wileyonlinelibrary.com.]
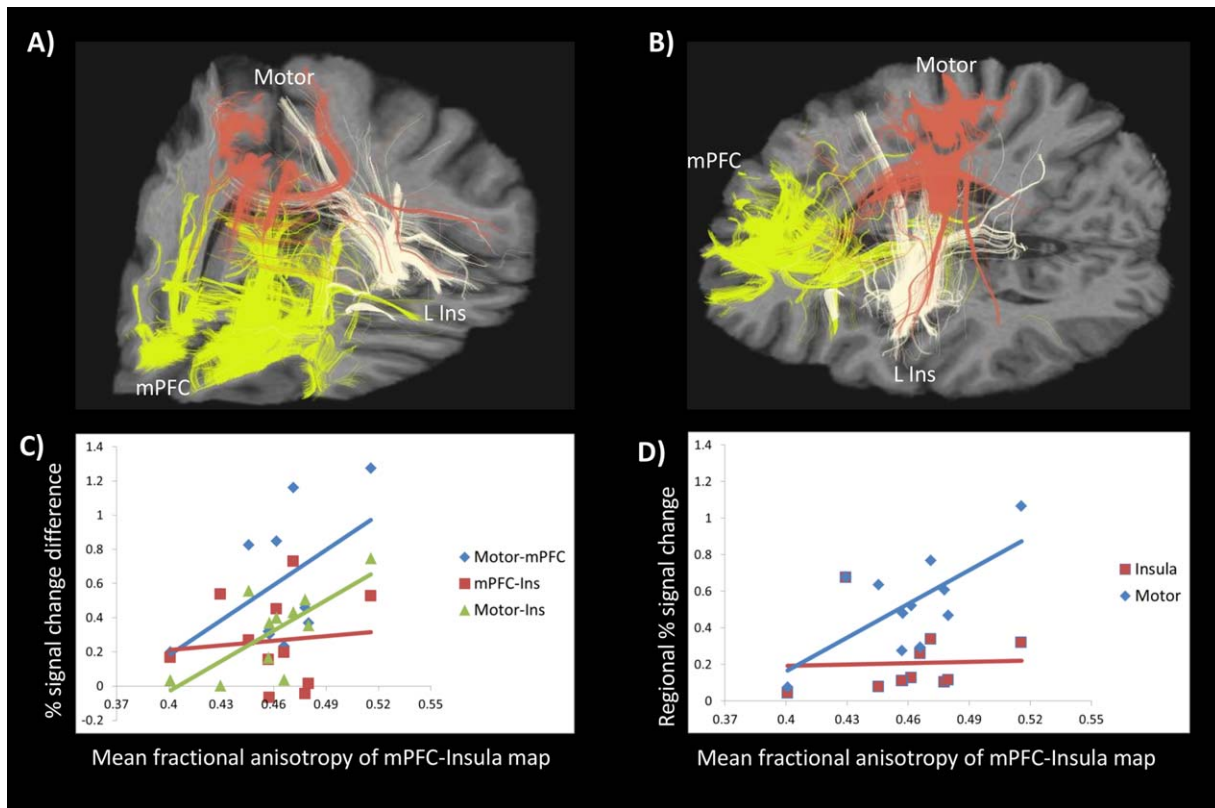
Figure 4.

Example of the three deterministic multi-tensor tractography models generated in an individual, as seen anteriorly (**A**) and sagittally (**B**), seeded from the mPFC (yellow), left insula (white), and motor cortex (red). The coordinates of the brain slices chosen for illustrative purposes, and which cut through the ROIs, are $x = 12$, $y = -10$, $z = 4$ in MNI space. mPFC-Insula connectivity is related to aversive signalling in the motor cortex, indicated by Pearson correlations between (**C**) connectivity strength (i.e. mean fractional anisotropy) of the mPFC-insula overlapping white matter map and the difference in signal changes between each region pair and (**D**) correlation between mPFC-insula connectivity and motor cortex activity during the aversive stimulus. [Color figure can be viewed in the online issue, which is available at wileyonlinelibrary.com.]

with mPFC entropy, or signal complexity (Fig. 2). CTQ scores also correlated with aversion-related brain responses. These results are additionally in support of our second hypothesis, when coupled with the finding that two regions common to all task- and rest-related measures, the left insula and motor cortex (Fig. 3), are also related to the strength of mPFC-insula connectivity (Fig. 4). Unexpectedly, it is interesting that only three regions (i.e. mPFC, LIns, and motor cortex) were identified here and not additional regions of the aversion-related network (e.g. posterior cingulate, thalamus, ventral striatum, amygdala), as might be anticipated. Also unexpected, only the mPFC-insula (and not the mPFC-motor or motor-insula) connectivity was correlated to aversion-related activity in the motor cortex, and the FA values from each of the connectivity maps were not correlated to CTQ scores. These issues are discussed further below. Taken together, these results suggest that some differences in resting state brain structure and function, as well as brain reactivity to aversive stimuli, may be related to the degree of NCEs in a healthy human population.

NCEs and mPFC Resting State Measures

Increased measures of individual NCEs were related to lower levels of mPFC Glu/NAA, while no relationship existed for Glu/NAA in the LIns, implying regional specificity for the mPFC (Fig. 2A; Table IB). Numerous studies in non-human animals have demonstrated an effect of early stressors on glutamatergic function in the mPFC [Ali et al., 2011; Llorente et al., 2012; Matrisciano et al., 2011] – as well as impacts in many other regions [Neto et al., 2012; Ryan et al., 2009; Waes et al., 2009]. Exposure to early life stressors in rats has revealed decreased glutamatergic measures in the rat mPFC using MRS [Llorente et al., 2012], altered glutamatergic (i.e., NMDA) receptor expression coupled with NMDA-linked impaired synaptic potentiation [Ali et al.,

2011; Judo et al., 2010; Matrisciano et al., 2011], and reduced mPFC cell firing rates [Ali et al., 2011]. Our findings are also in line with a general link between impaired glutamatergic function in the mPFC and animal models of acute and long-term stress, anxiety, and depression [Gutièrrez-Mecinas et al., 2011; Harvey and Shahid, 2012; Knox et al., 2010]. However, no previous studies have linked measures of early life stressors or NCEs and glutamatergic function in healthy humans, although many studies have investigated gluta-mate in the context of mood and anxiety disorders with con-sistent findings of reduced mPFC glutamate levels [Alcaro et al., 2010; Hettema et al., 2011; Nair and Singh Ajit, 2008; Riaza Bermudo-Soriano et al., 2012].

Alterations in intrinsic activity, particularly in the so-called default-mode network, have been linked to mood and anxi-ety disorders that are also associated with early life stress [Broyd et al., 2009; Northoff et al., 2011; Sylvester et al., 2012]. The current findings advance this notion by demonstrating that the degree of NCEs may impact resting state activity properties in the mPFC – a key region within the default-mode and affective processing networks [Daniels et al., 2011; Roy et al., 2012]. Increased instances of reported NCEs were related to increased measures of mPFC, but not insular, entropy (Fig. 2B; Table IC). This is consistent with prior find-ings showing that mPFC entropy measures are related to autonomic activity at rest [Ziegler et al., 2009] and that higher entropy or complexity is often, but not always, related to poorer functioning in mental disorders such as Alzheimer's or schizophrenia [Takahashi, 2013]. The link between NCEs, glutamate, and entropy complement and extend previous studies showing an effect of early life stressors on EEG fre-quency bands which predict signal entropy [Bruce et al., 2009; McFarlane et al., 2005], and prior results demonstrating an effect of stress on mPFC resting state activity [Molina et al., 2010; Philip et al., 2013a; Shin and Handwerger, 2009]. In addition, they support the idea that the development of intrinsic activity is likely important for healthy adult brain function, and that early life stressors or NCEs may act over time to constrain the range of variable responses in this regard [McIntosh et al., 2008; Raja Beharelle et al., 2012; Uhl-haas and Singer, 2011]. It is also important to note that our findings are in the eyes-closed (and not eyes-open) resting state period only. Although the mechanism for such a differ-ence is currently unclear, these findings are in line with our prior findings (Qin et al., 2012) and the recent work of others [Zhang et al., 2015] revealing clear differences in resting state activity between these two conditions and controversially suggesting that the eyes-closed condition may be somewhat closer to what is meant by a 'resting state'.

NCEs Are Correlated to an mPFC-Insula-Motor Cortex Network

Aversion-related brain responses were shown to be neg-atively correlated with CTQ scores during the anticipation of both a certain and uncertain shock, suggesting that peo-ple who self-report greater NCEs do not show the same neural reactivity as those reporting fewer NCEs (Fig. 3). Interestingly, although there is some evidence from the animal literature that 'safety' signals might contribute sig-nificantly to this correlation [Christianson et al., 2011; Fer-nando et al., 2014], we found the relationship between NCEs and signal changes related only to the aversive responsivity (Fig. 3F). Although our measure of NCEs neg-atively correlated with activity throughout the aversion network [Hayes and Northoff, 2011], the motor cortex and LIns were identified as key areas when considered in con-junction with mPFC measures of glutamate and signal complexity (Fig. 3E). Measures of combined mPFC gluta-mate/glutamine correlate positively with BOLD responses in task-positive regions [Duncan et al., 2011], fitting with the relationship seen between mPFC glutamate and aversion-related responses seen here. Moreover, these data are also consistent with the role of the mPFC as an integra-tive region that modulates and contextualizes cognitive-emotional responses to stimuli [Hayes et al., 2014; Roy et al., 2012]. Interestingly, fractional anisotropy of the mPFC-insula connectivity, an indirect measure of connec-tion strength, was correlated to aversion-related BOLD activity in the motor cortex but was not correlated to CTQ scores, suggesting that the association between NCEs and connectivity may be mediated by aversion-related activity in this case. This is not inconsistent with the notion that mPFC white matter volume may be altered in those with greater levels of NCEs [Hanson et al., 2012], and in fact future studies should include measures of NCEs in both healthy and clinical populations to investigate the possibil-ity of graded effects. It is worth noting that although most prior work has focused on alterations in the amygdala and hippocampus in people reporting NCEs [Dannlowski et al., 2012; Hart and Rubia, 2012], a meta-analysis of imaging studies on post-traumatic stress disorder found decreased activation in many of the regions identified here, including the insula and mPFC [Etkin and Wager, 2007]. Similarly, higher anxiety levels correlate with reduced activity changes in response to aversive stimuli in these regions [Drevets et al., 1995; Simpson et al., 2001; Zhao et al., 2007].

We found the mean fractional anisotropy of the white matter connection between the mPFC and left insula—an indicator of structural connectivity strength [Ben-Shachar et al., 2007; Khalsa et al., 2014]—to be positively correlated to aversion-related signal changes in motor cortex (Fig. 4). This finding is in line with prior work showing decreases in PFC white and grey matter volumes in healthy humans with more self-reported NCEs [Hanson et al., 2012] as well as a study on decision-making which showed increased functional connectivity between the mPFC and left anterior insula during the processing of affective context [Rudorf and Hare, 2014]. However, NCEs were not correlated to mPFC-insula structural connectivity directly, though they are correlated to insula and motor cortex signal changes,
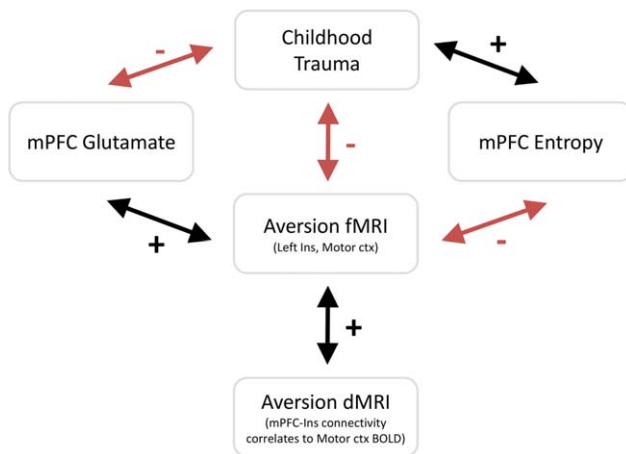
Figure 5.

Overview of study results showing relationship between CTQ scores, resting state measures, and aversion task responses. Green arrows denote a positive relationship and red negative. mPFC, medial prefrontal cortex. [Color figure can be viewed in the online issue, which is available at wileyonlinelibrary.com.]

suggesting that the relationship between NCEs and mPFC-insular-motor cortex signals is influenced indirectly via this structural connectivity. It is unclear why connections between the mPFC-motor cortex and insula-motor cortex appear unrelated to aversion-related signal changes (Fig. 4; Table II). However this might be related to the fact that these connections are mainly indirect through cortico-striatal-motor and cortico-thalamic pathways [Guye et al., 2003; Neggers et al., 2015]. Also, the insula is anatomically variable [Rosen et al., 2015] and its connections are regionally-selective (e.g. motor connectivity arises mainly from the posterior insula), but show generally strong connectivity to prefrontal regions [Cloutman et al., 2011]. Thus, our insular ROI, which included the entire region, may be better suited for uncovering relationships to the prefrontal cortex compared to many other regions. Regardless, our low sample size seems an unlikely candidate given the strength (mPFC-insula), or complete absence (mPFC-motor; insula-motor), of correlations (Table IIA,B).

Taken together, and in light of prior human and animal findings on the impact of early life stressors on brain structure and function, these findings (Fig. 5) support the evidence that a prefrontal-insular-motor cortex network is fundamentally involved in the processing of, and responsivity to, aversive stimuli and that this network can be shaped by NCEs.

LIMITATIONS AND CONCLUSION

There are a number of limitations of the current study. Firstly, although consistency of these results with those of the larger subgroups and across independent modalities point to their robustness, replication with a larger sample

is essential. Secondly, although one may question the reliability of the self-reporting of NCEs (via the CTQ), prior evidence into the validity of abuse reports supports their reliability [Chu et al., 1999]. Similarly, one may question the validity of concluding brain changes from CTQ scores in a non-clinical population given that participants were healthy at the time of the study. However, prior studies have observed physiological changes correlating with CTQ scores in healthy subjects [Carpenter et al., 2011; McFarlane et al., 2005], and in conjunction with our own, these findings may reflect the potential continuum-like impact of NCEs on brain and behavior in adulthood. Future studies which include both healthy and clinical-level subjects will be needed to outline this idea further. On the other hand, it is not possible in our current sample to rule out relationships between negative experiences in adulthood with the brain effects seen here, or to consider the possible impact of individual resiliency levels [Cisler et al., 2012]. Thirdly, although subjects were monitored for drowsiness during rsfMRI, we did not correlate levels of awareness with entropy values. Fourthly, given that the subjects did not rate their level of anxiety for the anticipation of the impeding shock, it is possible that the correlations seen here are more related to individual anxiety levels compared to aversive responding per se, especially as anxiety has been previously tied to NCEs [Huh et al., 2014]. Finally, subjects were recruited from the local student population and so, given the general class and educational structure of such a group, may not be representative of the population as a whole. Extending the study into different social contexts and specific patient populations is thus a desirable next step.

In conclusion, using a multimodal imaging dataset, it was shown that reported NCEs correlate with mPFC resting state dynamics and biochemistry, and are related to altered aversion-related neural responses and structural connectivity between the mPFC and LIns. Although it is merely speculation at this point, we suspect that under most conditions, the following findings likely reflect a poorer (i.e. nearer to pathological) overall response to aversive/stressful stimuli: (1) relatively lower aversion-related network responsivity to unpleasant stimuli, (2) lower resting state levels of mPFC glutamate, (3) increased mPFC entropy, and (4) alterations in mPFC white matter connectivity (though this appears indirect in the present study). This statement is made in light of the many animal and human studies (particularly those related to general aversive responding and anxiety and mood disorders) noted above. These results provide potential links between previous animal studies and clinical observations and give insight into the mechanisms by which early life experiences may impact upon brain function in adulthood.

ACKNOWLEDGMENTS

Garrett DD, Samanez-Larkin GR, MacDonald SWS, Lindenberger U, McIntosh AR, Grady CL (2013): Moment-to-moment brain signal variability: A next frontier in human brain mapping? Neurosci Biobehav Rev 37:610–624.

Gould F, Clarke J, Heim C, Harvey P, Majer M, Nemeroff C (2012): The effects of child abuse and neglect on cognitive functioning in adulthood. J Psychiatr Res 46:500–506.

Grant M, Cannistraci C, Hollon S, Gore J, Shelton R (2011): Childhood trauma history differentiates amygdala response to sad faces within MDD. J Psychiatr Res 45:886–895.

Gutièrrez-Mecinas M, Trollope A, Collins A, Morfett H, Hesketh S, Kersanté F, Reul J (2011): Long-lasting behavioral responses to stress involve a direct interaction of glucocorticoid receptors with ERK1/2-MSK1-Elk-1 signaling. Proc Natl Acad Sci U S A 108:13806–13811.

Guye M, Parker GJM, Symms M, Boulby P, Wheeler-Kingshott CAM, Salek-Haddadi A, Barker GJ, Duncan JS (2003): Combined functional MRI and tractography to demonstrate the connectivity of the human primary motor cortex in vivo. Neuroimage 19:1349–1360.

Hanson JL, Chung MK, Avants BB, Rudolph KD, Shirtcliff EA, Gee JC, Davidson RJ, Pollak SD (2012): Structural variations in prefrontal cortex mediate the relationship between early childhood stress and spatial working memory. J Neurosci 32:7917–7925.

Hart H, Rubia K (2012): Neuroimaging of child abuse: A critical review. Front Hum Neurosci 6:52.

Harvey BH, Shahid M (2012): Metabotropic and ionotropic glutamate receptors as neurobiological targets in anxiety and stress-related disorders: Focus on pharmacology and preclinical translational models. Pharmacol Biochem Behav 100:775–800.

Hauge ER, Berle JØ, Oedegaard KJ, Holsten F, Fasmer OB (2011): Nonlinear analysis of motor activity shows differences between schizophrenia and depression: A study using Fourier analysis and sample entropy. PLoS One 6:e16291.

Hayes DJ, Duncan NW, Wiebking C, Pietruska K, Qin P, Lang S, Gagnon J, Bing PG, Verhaeghe J, Kostikov AP, Schirrmacher R, Reader AJ, Doyon J, Rainville P, Northoff G, Gravel P (2013): GABA(A) receptors predict aversion-related brain responses: An fMRI-PET investigation in healthy humans. Neuropsychopharmacology 38:1438–1450.

Hayes DJ, Duncan NW, Xu J, Northoff G (2014): A comparison of neural responses to appetitive and aversive stimuli in humans and other mammals. Neurosci Biobehav Rev 45:350–368.

Hayes DJ, Northoff G (2011): Identifying a network of brain regions involved in aversion-related processing: A cross-species translational investigation. Front Integr Neurosci 5:1–21.

Hettema J, Kettenmann B, Ahluwalia V, McCarthy C, Kates W, Schmitt J, Silberg J, Neale M, Kendler K, Fatouros P (2011): Pilot multimodal twin imaging study of generalized anxiety disorder. Depress Anxiety 29:2010–209.

Howell BR, McCormack KM, Grand AP, Sawyer NT, Zhang X, Maestripieri D, Hu X, Sanchez MM (2013): Brain white matter microstructure alterations in adolescent rhesus monkeys exposed to early life stress: Associations with high cortisol during infancy. Biol Mood Anxiety Disord 3:21.

Howells FM, Stein DJ, Russell Va (2012): Childhood trauma is associated with altered cortical arousal: Insights from an EEG Study. Front Integr Neurosci 6:120.

Huh HJ, Kim SY, Yu JJ, Chae JH (2014): Childhood trauma and adult interpersonal relationship problems in patients with depression and anxiety disorders. Ann Gen Psychiatry 13: 26

Jahng JW, Ryu V, Yoo SB, Noh SJ, Kim JY, Lee JH (2010): Meso-limbic dopaminergic activity responding to acute stress is blunted in adolescent rats that experienced neonatal maternal separation. Neuroscience 171:144–152.

Judo C, Matsumoto M, Yamazaki D, Hiraide S (2010): Early stress exposure impairs synaptic potentiation in the rat medial pre-frontal cortex underlying contextual fear extinction. Neuroscience 169:1705–1714.

Kelly RE, Alexopoulos GS, Wang Z, Gunning FM, Murphy CF, Morimoto SS, Kanellopoulos D, Jia Z, Lim KO, Hoptman MJ (2010): Visual inspection of independent components: Defining a procedure for artifact removal from fMRI data. J Neurosci Methods 189:233–245.

Khalsa S, Mayhew SD, Chechlacz M, Bagary M, Bagshaw AP (2014): The structural and functional connectivity of the posterior cingulate cortex: Comparison between deterministic and probabilistic tractography for the investigation of structure-function relationships. Neuroimage 102 (Pt 1):118–127.

Kiem SA, Andrade KC, Spoormaker VI, Holsboer F, Czisch M, Sämann PG (2013): Resting state functional MRI connectivity predicts hypothalamus-pituitary-axis status in healthy males. Psychoneuroendocrinology 38:1338–1348.

Knox D, Perrine S, George S, Galloway M, Liberzon I (2010): Single prolonged stress decreases glutamate, glutamine, and creatine concentrations in the rat medial prefrontal cortex. Neuroscience 480:16–20.

Kuo J, Goldin P, Werner K, Heimberg R (2011): Childhood trauma and current psychological functioning in adults with social anxiety disorder. J Anxiety Disord 25:467–473.

Ladouceur A, Tessier J, Provencher B, Rainville P, Piché M (2012): Top-down attentional modulation of analgesia induced by heterotopic noxious counterstimulation. Pain 153:1755–1762.

Leemans A, Jones DK (2009): The B-matrix must be rotated when correcting for subject motion in DTI data. Magn Reson Med 61:1336–1349.

Liberzon I, King A, Britton J, Phan K (2007): Paralimbic and medial prefrontal cortical involvement in neuroendocrine responses to traumatic stimuli. Am J Psychiatry 164:1250–1258.

Llorente R, Villa P, Marco EM, Viveros MP (2012): Analyzing the effects of a single episode of neonatal maternal deprivation on metabolite profiles in rat brain: A proton NMR spectroscopy study. Neuroscience 201:12–19.

Lu S, Wei Z, Gao W, Wu W, Liao M, Zhang Y, Li W, Li Z, Li L (2013): White matter integrity alterations in young healthy adults reporting childhood trauma: A diffusion tensor imaging study. Aust N Z J Psychiatry 47:1183–1190.

Mailhot J-P, Vachon-Presseau E, Jackson PL, Rainville P (2012): Dispositional empathy modulates vicarious effects of dynamic pain expressions on spinal nociception, facial responses and acute pain. Eur J Neurosci 35:271–278.

Majer M, Nater U, Lin J, Capuron L, Reeves W (2010): Association of childhood trauma with cognitive function in healthy adults: A pilot study. BMC Neurol 10:61.

Marjanska M, Henry P-G, Auerbach EJ, Franc D, Mueller B, Ugurbil K, Lim KO (2007): Reproducibility of in vivo GABA quantification in anterior cingulate at 3 Tesla. Proc Intl Soc Mag Reson Med 15:1398.

Matrisciano F, Tueting P, Maccari S, Nicoletti F, Guidotti A (2011): Pharmacological activation of group-II metabotropic glutamate receptors corrects a schizophrenia-like phenotype induced by prenatal stress in mice. Neuropsychopharmacology 37:929–938.

McFarlane A, Clark CR, Bryant RA, Williams LM, Niaura R, Paul RH, Hitsman BL, Stroud L, Alexander DM, Gordon E (2005):

The impact of early life stress on psychophysiological, personality and behavioral measures in 740 non-clinical subjects. J Integr Neurosci 4:27–40.

McIntosh AR, Kovacevic N, Itier RJ (2008): Increased brain signal variability accompanies lower behavioral variability in development. PLoS Comput Biol 4:e1000106.

Mescher M, Merkle H, Kirsch J, Garwood M, Gruetter R (1998): Simultaneous in vivo spectral editing and water suppression. NMR Biomed 11:266–272.

Misić B, Mills T, Taylor MJ, McIntosh AR, Misic B (2010): Brain noise is task dependent and region specific. J Neurophysiol 104:2667–2676.

Molina ME, Isoardi R, Prado MN, Bentolila S (2010): Basal cerebral glucose distribution in long-term post-traumatic stress disorder. World J Biol Psychiatry 11:493–501.

Mueller S, Maheu F, Dozier M, Peloso E, Mandell D, Leibenluft E, Pine D, Ernst M (2010): Early-life stress is associated with impairment in cognitive control in adolescence: An fMRI study. Neuropsychologia 48:3037–3044.

Nair J, Singh Ajit S (2008): The role of the glutamatergic system in posttraumatic stress disorder. CNS Spectr 13:585–591.

Neggers SFW, Zandbelt BB, Schall MS, Schall JD (2015): Comparative diffusion tractography of cortico-striatal motor pathways reveals differences between humans and macaques. J Neurophysiol 113:2164–2172:jn.00569.2014.

Nelson E, Heath A, Madden P, Cooper M, Dinwiddie S, Bucholz K, Glowinski A, McLaughlin T, Dunne M, Statham D, Martin N (2002): Association between self-reported childhood sexual abuse and adverse psychosocial outcomes: Results from a twin study. Arch Gen Psychiatry 59:139–145.

Neto JB, Tiba P, Faturi C, de Castro-Neto E, da Graça Naffah-Mazacoratti M, de Jesus Mari J, de Mello M, Suchecki D (2012): Stress during development alters anxiety-like behavior and hippocampal neurotransmission in male and female rats. Neuropharmacology 62:518–526.

Northoff G, Wiebking C, Feinberg T, Panksepp J (2011): The "resting-state hypothesis" of major depressive disorder-A translational subcortical-cortical framework for a system disorder. Neurosci Biobehav Rev 35:1929–1945.

Paivio SC, Cramer KM (2004): Factor structure and reliability of the childhood trauma questionnaire in a Canadian undergraduate student sample. Child Abuse Negl 28:889–904.

Philip NS, Sweet LH, Tyrka AR, Price LH, Bloom RF, Carpenter LL (2013a): Decreased default network connectivity is associated with early life stress in medication-free healthy adults. Eur Neuropsychopharmacol 23:24–32.

Philip NS, Sweet LH, Tyrka AR, Price LH, Carpenter LL, Kuras YI, Clark US, Niaura RS (2013b): Early life stress is associated with greater default network deactivation during working memory in healthy controls: a preliminary report. Brain Imaging Behav 7:204–212.

Piché M, Arsenault M, Rainville P (2010): Dissection of perceptual, motor and autonomic components of brain activity evoked by noxious stimulation. Pain 149:453–462.

Provencher SW (1993): Estimation of metabolite concentrations from localized in vivo proton NMR spectra. Magn Reson Med 30:672–679.

Provencher SW (2001): Automatic quantitation of localized in vivo 1H spectra with LCModel. NMR Biomed 14:260–264.

Qazi AA, Radmanesh A, O'Donnell L, Kindlmann G, Peled S, Whalen S, Westin C-F, Golby AJ (2009): Resolving crossings in the corticospinal tract by two-tensor streamline tractography:

Method and clinical assessment using fMRI. Neuroimage 47 (Suppl 2):T98–106.

Qin P, Duncan NW, Wiebking C, Gravel P, Lyttelton O, Hayes DJ, Verhaeghe J, Kostikov A, Schirrmacher R, Reader AJ, Northoff G (2012): GABAA receptors in visual and auditory cortex and neural activity changes during basic visual stimulation. Front Hum Neurosci 6:1–13.

Raja Beharelle A, Kovačević N, McIntosh AR, Levine B (2012): Brain signal variability relates to stability of behavior after recovery from diffuse brain injury. Neuroimage 60:1528–1537.

Reiss S, Peterson R, Gursky D, McNally R (1986): Anxiety sensitivity, anxiety frequency and the prediction of fearfulness. Behav Res Ther 24:1–8.

Riaza Bermudo-Soriano C, Perez-Rodriguez MM, Vaquero-Lorenzo C, Baca-Garcia E (2012): New perspectives in glutamate and anxiety. Pharmacol Biochem Behav 100:752–774.

Richman JS, Moorman JR (2000): Physiological time-series analysis using approximate entropy and sample entropy. Am J Physiol Hear Circ Physiol 278:H2039–H2049.

Rosen A, Chen D, Hayes DJ, Davis K, Hodaie M (2015): A neuroimaging strategy for the three dimensional in vivo anatomical visualization and characterization of insular gyri. Stereotact Funct Neurosurg 93:255–264.

Roy M, Shohamy D, Wager TD (2012): Ventromedial prefrontal-subcortical systems and the generation of affective meaning. Trends Cogn Sci 16:147–156.

Rudorf S, Hare TA (2014): Interactions between dorsolateral and ventromedial prefrontal cortex underlie context-dependent stimulus valuation in goal-directed choice. J Neurosci 34:15988–15996.

Ryan B, Musazzi L, Mallei A, Tardito D, Gruber S, El Khoury A, Anwyl R, Racagni G, Mathe A, Rowan M, Popoli M (2009): Remodelling by early-life stress of NMDA receptor-dependent synaptic plasticity in a gene-environment rat model of depression. Int J Neuropsychopharmacol 12:553–559.

Shin LM, Liberzon I (2010): The neurocircuitry of fear, stress, and anxiety disorders. Neuropsychopharmacology 35:169–191.

Shin L, Handwerger K (2009): Is posttraumatic stress disorder a stress induced fear circuitry disorder? J Trauma Stress 22:409–415.

Shin L, Orr S, Carson M, Rauch S, Macklin M, Lasko N, Peters P, Metzger L, Dougherty D, Cannistraro P, Alpert N, Fischman A, Pitman R (2004): Regional cerebral blood flow in the amygdala and medial prefrontal cortex during traumatic imagery in male and female Vietnam veterans with PTSD. Arch Gen Psychiatry 61:168–176.

Simpson JR, Drevets WC, Snyder AZ, Gusnard DA, Raichle ME (2001): Emotion-induced changes in human medial prefrontal cortex. II. During anticipatory anxiety. Proc Natl Acad Sci U S A 98:688–693.

Smith SM, Jenkinson M, Woolrich MW, Beckmann CF, Behrens TEJ, Johansen-Berg H, Bannister PR, De Luca M, Drobnjak I, Flitney DE, others (2004): Advances in functional and structural MR image analysis and implementation as FSL. Neuroimage 23:S208–S219.

Sylvester CM, Corbetta M, Raichle ME, Rodebaugh TL, Schlaggar BL, Sheline YI, Zorumski CF, Lenze EJ (2012): Functional network dysfunction in anxiety and anxiety disorders. Trends Neurosci 35:1–9.

Takahashi T (2013): Complexity of spontaneous brain activity in mental disorders. Prog Neuropsychopharmacol Biol Psychiatry 45:258–266.

Thomaes K, Dorrepaal E, Draijer N, de Ruiter M, Elzinga B, van Balkom A, Smit J, Veltman D (2012): Treatment effects on

insular and anterior cingulate cortex activation during classic and emotional Stroop interference in child abuse-related complex post-traumatic stress disorder. Psychol Med 42:2337–2349.

Van Tol M, Demenescu L, van der Wee N, Kortekaas R, Marjan M, Boer J, Renken R, van Buchem M, Zitman F, Aleman A, DJ V (2012): Functional magnetic resonance imaging correlates of emotional word encoding and recognition in depression and anxiety disorders. Biol Psychiatry 71:593–602.

Turecki G, Ernst C, Jollant F, Labonte B, Mechawar N, Labonté B (2012): The neurodevelopmental origins of suicidal behavior. Trends Neurosci 35:14–23.

Uhlhaas PJ, Singer W (2011): The development of neural synchrony and large-scale cortical networks during adolescence: Relevance for the pathophysiology of schizophrenia and neurodevelopmental hypothesis. Schizophr Bull 37:514–523.

Waes V Van, Enache M, Zuena A (2009): Ethanol attenuates spatial memory deficits and increases mGlu1a receptor expression in the hippocampus of rats exposed to prenatal stress. Alcohol Clin Exp Res 33:1346–1354.

Willer JC (1977): Comparative study of perceived pain and nociceptive flexion reflex in man. Pain 3:69–80.

Woolrich M, Jbabdi S, Patenaude B, Chappell M (2009): Bayesian analysis of neuroimaging data in FSL. Neuroimage 45:S173–S186.)01204-4.

Zhang D, Liang B, Wu X, Wang Z, Xu P, Chang S, Liu B, Liu M, Huang R (2015): Directionality of large-scale resting-state brain networks during eyes open and eyes closed conditions. Front Hum Neurosci 9:81

Zhao X-H, Wang P-J, Li C-B, Hu Z-H, Xi Q, Wu W-Y, Tang X-W (2007): Altered default-mode network activity in patient with anxiety disorders: an fMRI study. Eur J Radiol 63:373–378.

Ziegler G, Dahnke R, Yeragani VK, Bär K-J (2009): The relation of ventromedial prefrontal cortex activity and heart rate fluctuations at rest. Eur J Neurosci 30:2205–2210.